J Solid State Electrochem (2005) 9: 1–9
DOI 10.1007/s10008-004-0528-7

ORIGINAL PAPER

M. Łukaszewski · M. Grdeń · A. Czerwiński

Cyclic voltammetric behavior of Pd–Pt–Rh ternary alloys

Received: 9 November 2003 / Accepted: 11 March 2004 / Published online: 27 April 2004

Abstract The electrochemical behavior of Pd–Pt–Rh alloys has been investigated using cyclic voltammetry (CV). The alloys were prepared by electrochemical co-deposition as limited volume electrodes (less than 1 μm in thickness). The morphology of the alloy surface and bulk compositions were examined by the SEM/EDAX method. Surface oxides generation (oxygen adsorption) and oxides reduction (oxygen desorption) currents together with hydrogen adsorption and hydrogen absorption signals can be distinguished on CV curves. During potential cycling through the full hydrogen–oxygen potential range Rh and Pd are preferentially dissolved, which is reflected in a dramatic transformation in the voltammogram shape. The composition changes involve not only the surface but also some atomic layers beneath the surface.

Keywords Ternary noble metal alloys · Limited volume electrodes · Cyclic voltammetry

Introduction

Studies on the electrochemistry of noble metal alloys have mainly been devoted to their electrocatalytic properties. These systems have provided many valuable data about the mechanism of electrocatalytic processes. The mixtures of elements with different electrochemical properties, which were found to be very useful in the explanation of various phenomena in electrocatalysis such as synergistic effects based on a third body or electrocatalysis effects, exhibit especially interesting behavior. Most such investigations have been carried out for binary noble metal systems (see e.g. [1, 2, 3, 4, 5, 6]) and the increasing number of reports provides similar data for alloys containing more than two elements, e.g. ternary alloys [7, 8, 9, 10, 11, 12, 13, 14, 15, 16, 17]. We have chosen the ternary Pd–Pt–Rh system as a mixture of elements with various electrochemical properties in order to explore the basic electrochemistry of ternary alloys composed exclusively of noble metals.

Platinum group metals are known to electrochemically adsorb hydrogen at potentials positive to the reversible hydrogen potential [18, 19]. Pd can also absorb hydrogen while for Pt and Rh bulk hydrogen dissolution is negligible [20]. Thus, mixing of Pd with such elements as Pt or Rh causes weakening alloy ability to absorb hydrogen [20, 21, 22]. The only exception is a system containing ca. 5–7 at.% of Rh but with a further increase in Rh content, however, the alloy capacity for hydrogen absorption sharply decreases [20, 23]. At sufficiently high potentials electrooxidation of the surface of noble metals occurs, involving the formation of surface oxides (oxygen adsorption) and the electrochemical dissolution of the electrode material. The processes of surface oxides generation and reduction on Rh electrode proceed at potentials markedly lower than those on Pd and Pt. On the other hand, Pt is much more inert in the process of electrochemical dissolution than Pd and Rh [18, 24].

In the investigations of the electrochemical behavior of noble metals and their alloys cyclic voltammetry (CV) has been established as a powerful in situ technique. It has been demonstrated that for electrodes of this type the voltammogram recorded under given experimental conditions is an electrochemical fingerprint of the sample studied [18, 24, 25, 26, 27]. Recently, the use of limited volume electrodes (LVEs) has allowed the examination of the electrochemistry of hydrogen-absorbing Pd

M. Łukaszewski · M. Grdeń · A. Czerwiński (✉)
Department of Chemistry, Warsaw University,
Pasteura 1, 02-093 Warsaw, Poland
E-mail: aczerw@chem.uw.edu.pl
Tel.: +48 22 8220211
Fax: +48 22 8225996

M. Łukaszewski · A. Czerwiński
Industrial Chemistry Research Institute,
Rydygiera 8, 01-793 Warsaw, Poland

alloys in the full hydrogen–oxygen potential range [27, 28, 29, 30].

In this paper we present the results of the studies on electrochemical behavior of ternary Pd–Pt–Rh alloys under conditions of cyclic voltammetric experiments. We have paid attention to alloy electrochemical ageing as well as to some aspects of the processes of hydrogen adsorption and absorption.

Experimental

Pd–Pt–Rh alloys of limited volume were deposited potentiostatically on gold wires (99.9%, 0.5 mm diameter) from a bath containing $PdCl_2$, H_2PtCl_6, $RhCl_3$ and HCl. The thickness of the deposited alloy layers was in the range 0.20–0.60 μm. The roughness factor of the deposit, as estimated from measurements of the surface oxides reduction charge [18], was ca. 100–350. Bulk compositions of the alloys were analyzed using an EDAX analyzer (EDR-286) coupled with a LEO 435VP scanning electron microscope. All alloys compositions given in this work are bulk compositions expressed in atomic percentages.

All experiments were performed at room temperature in 0.5 M H_2SO_4 solution deoxygenated using an Ar stream. A three-electrode cell was used with $Hg|Hg_2SO_4|0.5$ M H_2SO_4 as the reference electrode and a Pt gauze as the auxiliary electrode. All potentials are recalculated with respect to the SHE.

Results and discussion

General voltammetric behavior of Pd–Pt–Rh alloys

Figure 1a presents cyclic voltammograms for fresh Pd–Pt–Rh alloys with various bulk compositions recorded in the full hydrogen–oxygen potential range. Their general shape is similar to CV curves characteristic for pure Pd, Pt, and Rh electrodes presented for comparison in Fig. 1b. On the voltammograms one can distinguish hydrogen adsorption and hydrogen absorption signals (the hydrogen region—I), then a potential range free from faradaic processes (the double layer charging region—II), followed by surface oxides generation (oxygen adsorption) and oxides reduction (oxygen desorption) currents (the oxygen region—III). According to the method of surface composition analysis of noble metal binary alloys [18, 24, 25, 26, 27], the position of the oxygen desorption peak is a linear function of the surface alloy composition. Unfortunately, in the case of a ternary system it is impossible to use the same method for quantitative estimation of the surface composition. Thus, we can draw mainly qualitative conclusions about the surface composition on the basis of the shapes of CV curves. Such an analysis is possible owing to the fact that the voltammograms for pure Pd, Pt and Rh electrodes differ markedly from each other with respect to the region of oxygen adsorption, the potential of the oxygen desorption peak, and the appearance of the region where hydrogen sorption takes place [18, 24].

Various courses of CV curves in the oxygen as well as the hydrogen region obtained for Pd–Pt–Rh samples with various bulk component proportions indicate that the alloy surface compositions also differ from each other. In particular, the shape of the CV curve for alloy (1) suggests high surface concentration of Rh. The major differences from a CV response for pure Rh are: an additional current signal (a) in the hydrogen region and a wider potential range of hydrogen peaks (b) together with the shift of the surface oxides reduction peak (c) towards higher potential values. The latter effect can be linked to the presence of Pd and Pt atoms on the electrode surface. In the case of samples (2) and (3) the surface properties are closer to those of Pd–Pt alloys [25, 26, 27, 28], with a higher potential of peak (c), probably due to a higher Pd and Pt surface content. Various potentials of the onset of the surface oxidation process and oxides reduction (oxygen desorption) peaks should be noted. Interestingly, in the case of the relatively Rh-rich alloy (1) the process of surface oxides formation starts at a potential as low as that for pure Rh. As it can be seen in Fig. 1a, a single peak of surface oxides reduction (c) was observed for all these electrodes indicating phase homogeneity of the alloy surface [18].

The processes of electrochemical ageing

Figure 2a presents a series of CV curves for a Pd–Pt–Rh alloy (with initial bulk composition 56.5 at.% Pd, 8.0 at.% Pt, 35.5 at.% Rh) subjected to electrochemical ageing, i.e. cycling in the full hydrogen–oxygen potential range (−0.05 to 1.35 V, scan rate 0.1 V s^{-1}). It is known that during such a procedure one can expect alloy surface enrichment with components that are more resistive to the process of electrochemical dissolution, occurring at each scan through potentials of the oxygen region. It can be seen that the course of the voltammogram undergoes dramatic changes concerning both the hydrogen and oxygen region. Particularly striking is the continuous positive shift of surface oxides reduction peak, which suggests that surface composition is strongly altered. With the progress of the ageing process (i.e. when the number of potential cycles increases) the voltammogram transforms to that similar to Pd–Pt alloys [25, 26, 27, 28], without significant influence of Rh atoms. A similar effect was also observed for binary Pt-Rh alloys, where the voltammogram after long potential cycling resembled the CV curve for a pure Pt electrode [18, 24], indicating on low Rh concentration on the electrochemically aged alloy surface. The effect of surface composition changes occurs simultaneously with the decrease in the real surface area of the electrode indicated by the decrease in oxides reduction and generation currents. As it was reported in the literature [31, 32], the surface roughness of noble metal electrodes

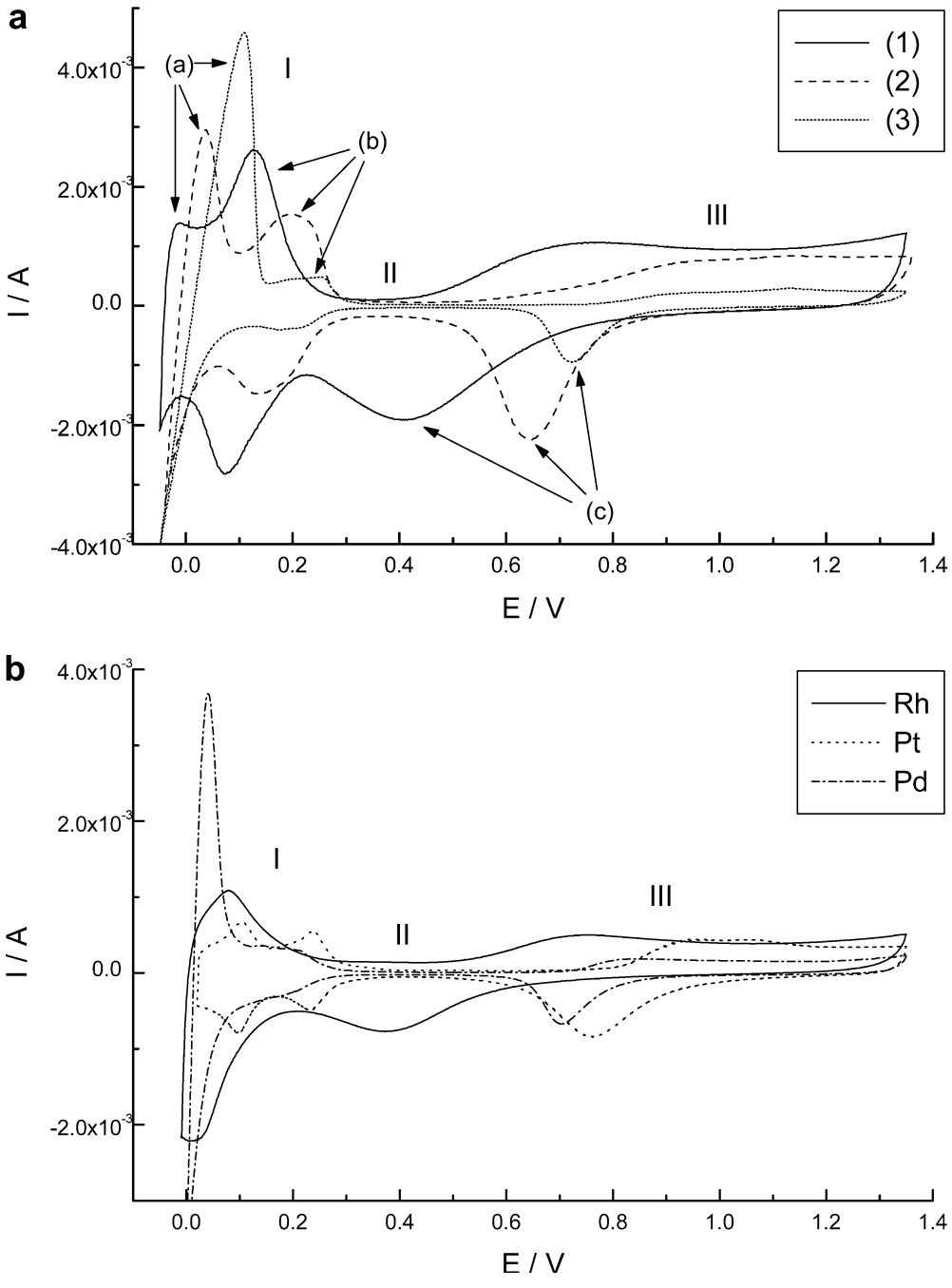

Fig. 1 Cyclic voltammograms recorded in the full hydrogen–oxygen potential range, scan rate 0.1 V s^{-1}. (**a**) Fresh Pd–Pt–Rh alloy electrodes, bulk compositions: (1) 56.5 at.% Pd, 8.0 at.% Pt, 35.5 at.% Rh; (2) 81.0 at.% Pd, 6.3 at.% Pt, 12.7 at.% Rh; (3) 89.2 at.% Pd, 4.9 at.% Pt, 5.9 at.% Rh. (**b**) Pure Pd, Pt, and Rh electrodes

subjected to the procedure of potential cycling through the oxygen region may increase or decrease and the tendency depends on the parameters applied in a cyclic voltammetric experiment. It appears that the latter case takes place here. We have already reported on such type of behavior for Pd-Au binary alloys [33]. It should be stressed that at all stages of Pd–Pt–Rh electrodes ageing only one symmetrical peak of surface oxides reduction was observed, which means that the alloy surface remained homogeneous [18].

The electrochemical ageing of Pd–Pt–Rh alloys rich in Pd (Fig. 2b) proceeded without such a dramatic evolution of voltammogram shape as that shown in Fig. 2a, probably due to much lower initial Rh content (initial bulk composition 83.0 at.% Pd, 11.0 at.% Pt and 6.0 at.% Rh). However, the general trends were similar to those described above, namely: the decrease in real surface area and the shift of oxygen desorption peak towards higher potentials. Interestingly, a splitting of hydrogen peak (a) occurred in the absorption region. This might indicate some kind of bulk separation into two phases exhibiting different absorption characteristics.

Scanning electron microscope (SEM) observations confirm that during the potential cycling procedure the alloy surface is altered. Two kinds of effects can be

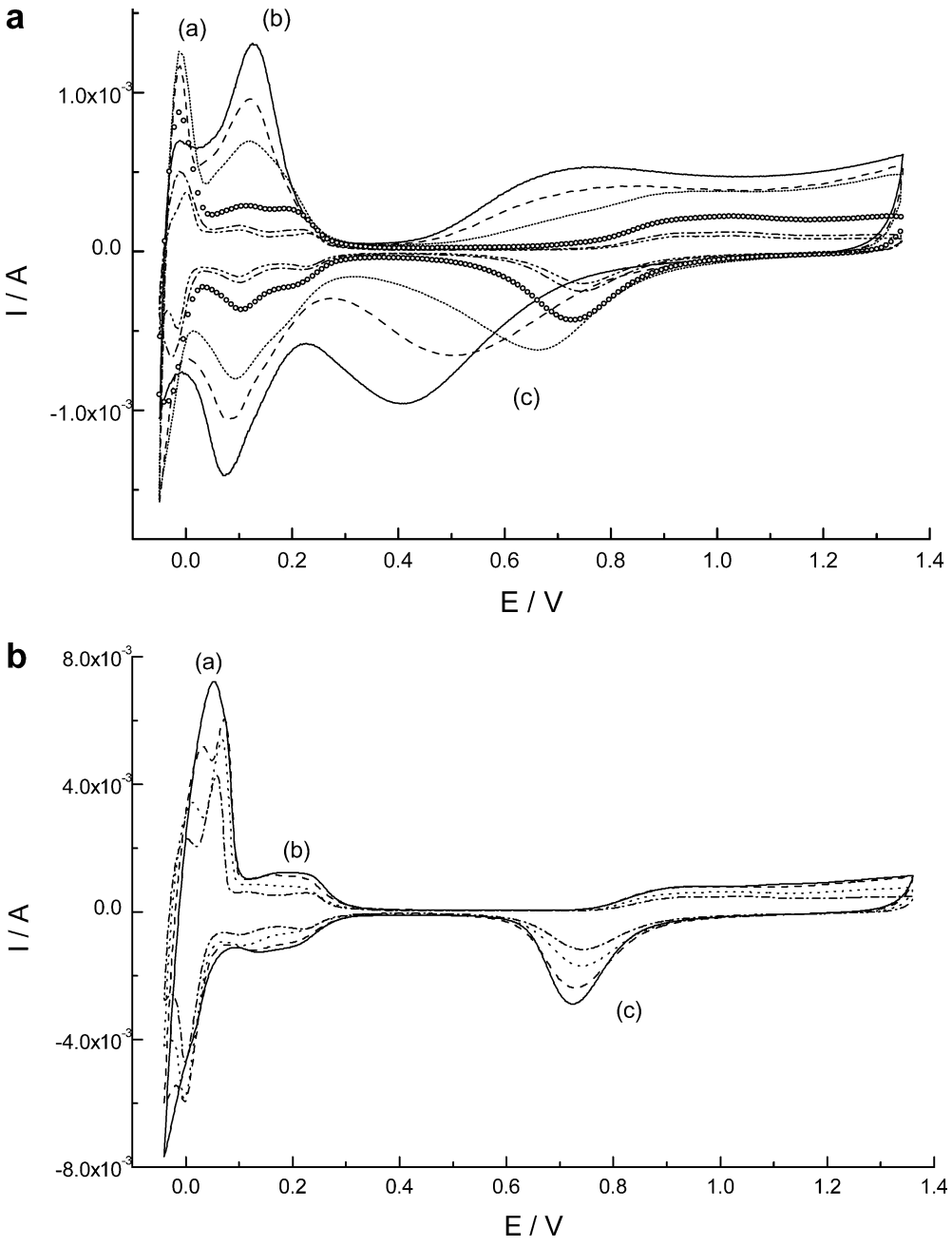

Fig. 2 Cyclic voltammograms for Pd–Pt–Rh alloys subjected to potential cycling in the full hydrogen–oxygen potential range, scan rate 0.1 V s^{-1}.**a** Initial alloy composition (in the bulk): 56.5 at.% Pd, 8.0 at.% Pt, 35.5 at.% Rh. (—) scan 1, (---) scan 50, (···) scan 100, (○○○) scan 200, (-·-·-) scan 400, (-··-··-) scan 600. **b**Initial alloy composition (in the bulk): 83.0 at.% Pd, 11.0 at.% Pt, 6.0 at.% Rh. (—) scan 1, (---) scan 55, (···) scan 135, (-·-·-) scan 295

distinguished. First, the oxygen sorption/desorption processes accompanied by metal dissolution and subsequent recrystallization lead to changes in the size of crystallites, and consequently, in the surface roughness (compare Fig. 3a and b). Second, hydrogen penetration into the bulk of the electrode occurring during polarization to hydrogen absorption potentials causes an increase in sample volume, together with cracking (compare Fig. 3c and d), since for Pd and Pd-rich alloys the lattice parameter increases due to the formation of the hydride phase [20, 34].

Figures 4a and b present the influence of the number of potential cycles (N) on the values of total charge of hydrogen oxidation peaks (Q^{H}_{ox}), charge of the reduction of the surface oxides (Q^{O}_{red}) and potential of the surface oxides reduction peak (E_p) for alloys containing ca. 56–58% Pd, 8% Pt and 34–36% Rh. One should note that Q^{O}_{red} values (see Fig. 4a) decrease monotonically, with a rapid drop during the initial 200 cycles, while for Q^{H}_{ox} values (see Fig. 4b) there is a plateau or even an increase for cycles ca. 20–80, followed by a further sharp decrease. After ca. 250 potential cycles both Q^{O}_{red} and Q^{H}_{ox} values decrease slowly.

These changes are linked to variations in E_p values, indicating modifications of the surface alloy composition [18, 24]. A comparison of Q^{H}_{ox}–N,Q^{O}_{red}–N and E_p–N plots shows that the most dramatic changes in Q^{O}_{red} and Q^{H}_{ox} values could be linked to the strong positive shift of peak potential, E_p. This effect suggests that at this stage of electrochemical treatment Rh is dissolved

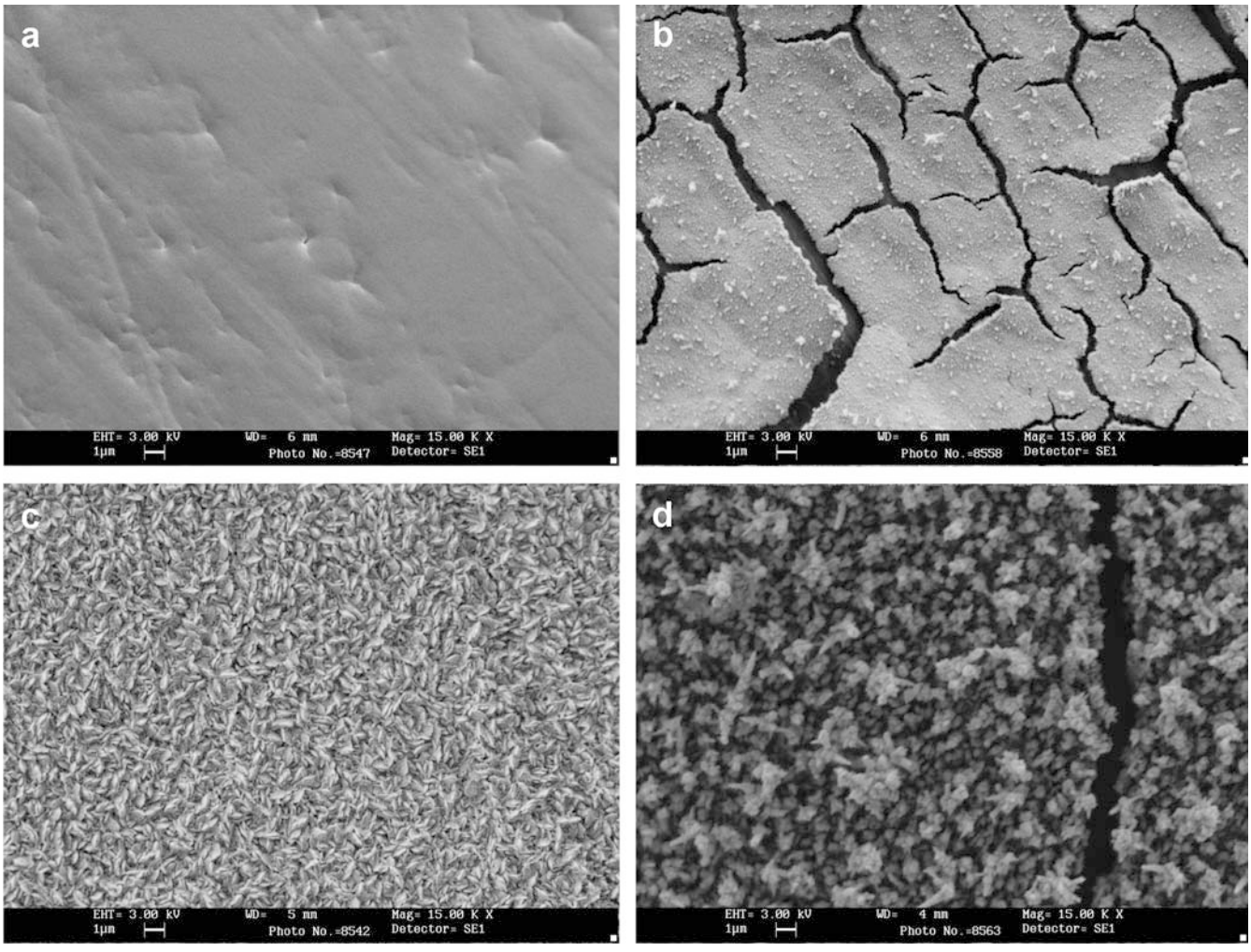

Fig. 3 SEM images taken for Pd–Pt–Rh alloys: a fresh alloy containing in the bulk 84.3 at.% Pd, 6.8 at.% Pt, 8.9 at.% Rh (**a**) and after 100 cycles (**b**); a fresh alloy containing in the bulk 91.6 at.% Pd, 2.4 at.% Pt, 6.0 at.% Rh (**c**) and after 130 cycles (**d**). Potential cycling range −0.05–1.35 V; scan rate 0.1 V s^{-1}

from the surface. Moreover, this process is also associated with the decrease in real surface area.

Table 1 presents a comparison of the initial and final (after number of cycles indicated) bulk alloy composition for three representative samples, determined using the EDAX method. Since significant changes in composition can be detected by this technique, examining thickness of the order of thousand atomic layers, it means that both Rh and Pd are removed from the bulk of the alloy (at least from layers close to the surface) as metals less resistive to electrochemical dissolution than Pt [18, 35]. It should be noted that the results of EDAX analysis for heavy elements, such as Pd, Pt and Rh are independent of the chemical state of the elements. Thus, any passivation processes occurring during electrode ageing could not influence the EDAX results.

The composition changes detected by EDAX measurements indicate that, although one cannot exclude the possibility of a redeposition in cathodic scans of some amount of previously dissolved metals, a major part of the dissolved metals is irreversibly removed from the electrode. It should be noted that under given conditions the components that dissolve more easily can also be expected to be reduced with a greater difficulty. As a result the redeposition process is limited and does not alter the tendency to continuous enrichment of the electrode surface with electrochemically less soluble (more noble) elements. Moreover, continuous changes in the potential of the surface oxides reduction peak without any splitting or new peaks growing suggest that even if redeposition occurs the surface of the electrode remains homogenous. In the case of significant Rh redeposition one could expect the formation of a new Rh-rich surface phase, which should lead to an additional surface oxides reduction peak appearing at lower potentials. Such a phenomenon has not been observed. On the other hand, a partial cathodic redeposition of dissolved metal might play a certain role in the surface morphology changes during potential cycling reflected in SEM images (Figs. 3a–d).

After a long period of potential cycling (for $N > 250$) mainly Pd dissolution takes place as indicated in Fig. 4a or b by a slow positive drift of E_p until practically a

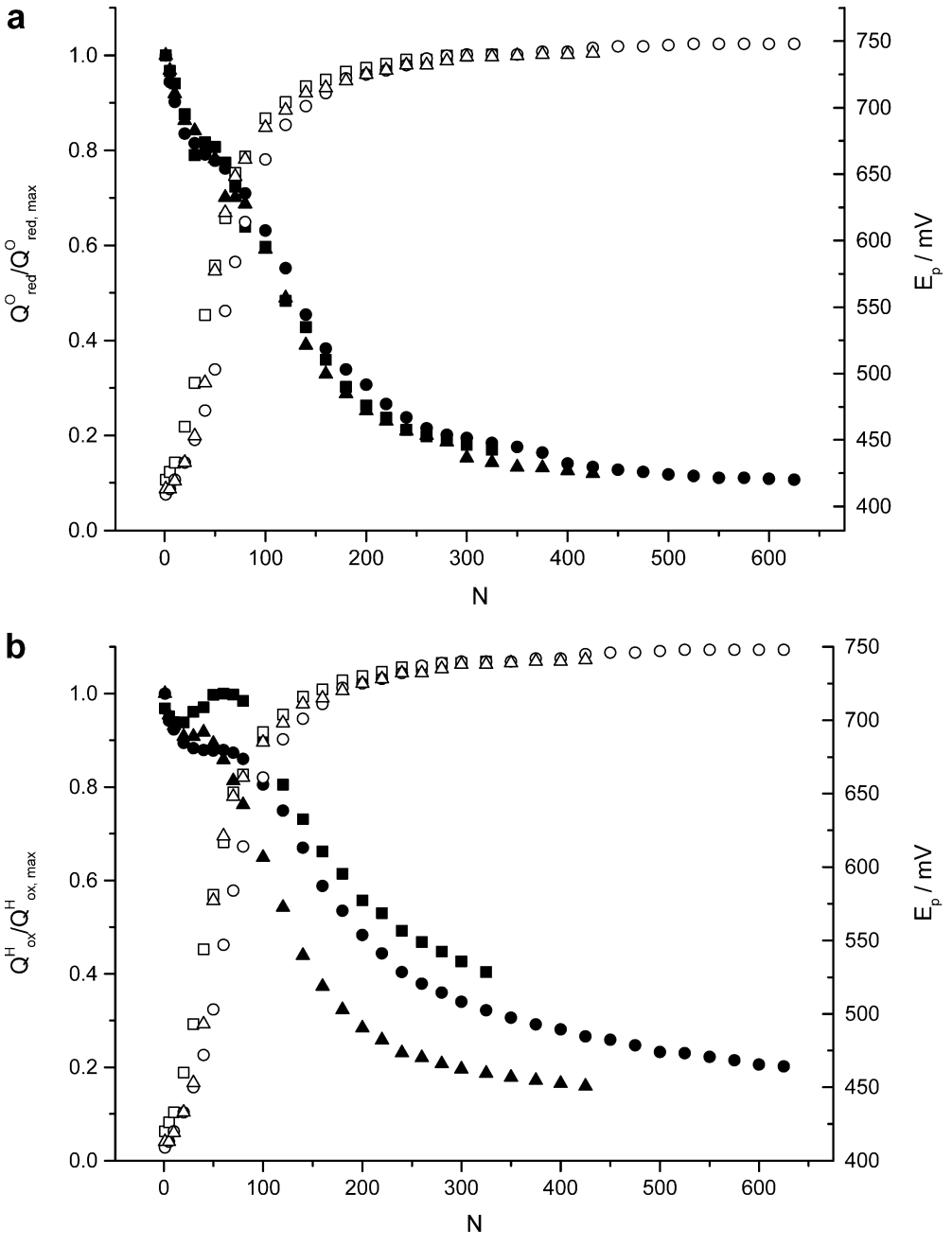

Fig. 4 Values of the surface oxides reduction charge (**a**) and the total hydrogen oxidation charge (**b**), expressed as their ratio to maximum values, $Q^{O}_{red}/Q^{O}_{red,\,max}$ and $Q^{H}_{ox}/Q^{H}_{ox,\,max}$ (filled symbols), and peak potential, E_p (empty symbols) versus number of potential cycles, N (potential range −0.05–1.35 V; scan rate 0.1 V s^{-1}) for Pd–Pt–Rh alloys with initial bulk compositions: ■,□ 57.5 at.% Pd, 8.2 at.% Pt, 34.3 at.% Rh; ●, ○ 56.5 at.% Pd, 8.0 at.% Pt, 35.5 at.% Rh; ▲, Δ 58.0 at.% Pd, 8.1 at.% Pt, 33.9 at.% Rh

stationary surface composition is reached. The fact that even after a long period of electrochemical treatment the potential of the surface oxides reduction peak remains slightly lower than that on pure Pt suggests the existence on the surface of not only Pt but also Pd and/or Rh atoms. Such a state could be maintained if the electrode surface was continuously supplied with Pd and/or Rh atoms transported from the bulk of the alloy by

Table 1 Bulk compositions of fresh and aged Pd–Pt–Rh alloys

Sample	Alloy thickness (μm)	Electrode state	Bulk composition		
			% at. Pd	% at. Pt	% at. Rh
1.	0.38 ± 0.04	Fresh electrode	57.5 ± 0.7	8.2 ± 0.3	34.3 ± 0.6
		After 370 cycles	28.5 ± 5.7	65.6 ± 5.8	6.0 ± 0.7
2.	0.20 ± 0.02	Fresh electrode	56.2 ± 0.7	8.0 ± 0.5	35.8 ± 0.4
		After 475 cycles	13.0 ± 2.6	83.9 ± 3.2	3.1 ± 1.1
3.	0.42 ± 0.04	Fresh electrode	56.5 ± 0.9	8.0 ± 0.2	35.5 ± 0.9
		After 625 cycles	11.4 ± 2.9	83.6 ± 5.9	5.0 ± 1.3

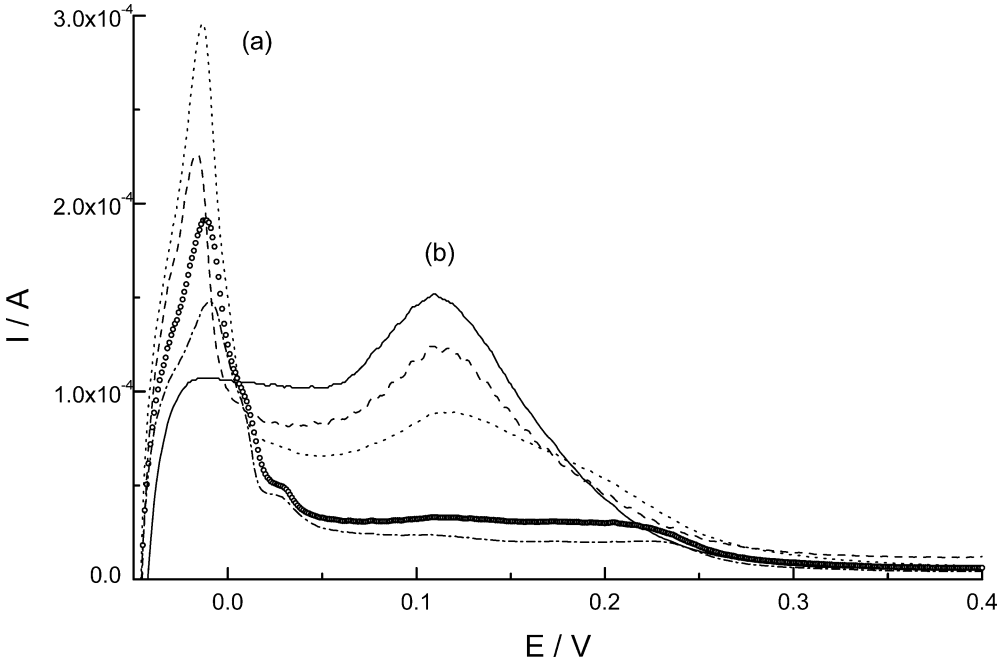

Fig. 5 Cyclic voltammograms for a Pd–Pt–Rh electrode (initial bulk composition 57.5 at.% Pd, 8.2 at.% Pt, 34.3 at.% Rh) recorded at 0.01 V s^{-1} after 300 s of polarization at −0.05 V for various stages of electrochemical treatment (potential cycling in the range −0.05–1.35 V; scan rate 0.1 V s^{-1}). Total number of potential cycles applied: (—) 1, (---) 40, (···) 90, (○○○) 190, (-·-·-) 290

diffusion. A similar situation has been reported in the literature [36] for the Pd–Au system.

Hydrogen adsorption and absorption

In Fig. 1a two kinds of current signals—denoted as (a) and (b)—can be seen below 0.3 V, reflecting the alloy's capability for hydrogen electrosorption. Since Pd ternary alloys absorb hydrogen [21, 22], we might expect the oxidation processes of both adsorbed and absorbed hydrogen to contribute to hydrogen anodic signals on voltammograms recorded for Pd–Pt–Rh alloys. One should note that peak (a) is particularly high on CV curves for alloys rich in Pd in the bulk (see curve 3 in Fig. 1a), which are characterized by a relatively high absorption capacity [20, 21, 22]. This suggests that this signal has a significant contribution from the oxidation of absorbed hydrogen. Signal (b), located at higher potentials, can be attributed to the oxidation of mainly adsorbed hydrogen.

As can be seen in Fig. 2a, peak (a) current reaches a maximum value for $50 < N < 100$, which corresponds to the region of Q^{H}_{ox}–N dependence, where a plateau or maximum exists (see Fig. 4b). Since the shape of the Q^{O}_{red}–N dependence (Fig. 4a) suggests a continuous decrease in real surface area with N, the increase in peak (a) current confirms that this signal originates mainly from oxidation of hydrogen absorbed in the bulk of the alloy, not just from surface processes alone.

After comparison with the E_p–Ndependence, we can link the maximum from the Q^{H}_{ox}–N plot (Fig. 4b) to a decrease in Rh content, at least in the alloy surface. These composition changes can improve hydrogen absorption into alloy by:

1. Removal of Rh atoms from the electrode surface. Fig. 1a indicates that the surface of a fresh alloy is strongly enriched with Rh. This Rh layer can generate a barrier, which blocks a surface stage of hydrogen insertion into the bulk of the alloy, i.e. blocks the reaction $H_{ads} \rightarrow H_{abs}$. Thus, Rh dissolution could strongly improve hydrogen absorption due to surface changes regardless of changes in the bulk alloy composition.
2. Dissolution of Rh from the bulk of the alloy during initial potential cycles, confirmed by the EDAX results. Because of a small electrode thickness the region involved with composition changes might be relatively large with respect to the sample volume. It produces alloys containing relatively more Pd in the bulk with respect to the sum of other elements, i.e. Pt and Rh. It is known that hydrogen absorption in ternary Pd–Pt–Rh alloys decreases with an increase in the amount of Pt and/or Rh [21, 22].

These changes in the alloy composition could facilitate hydrogen absorption in the alloy both kinetically and thermodynamically. At the moment, however, it is difficult to conclude which factor, surface or bulk Rh dissolution, is more important.

The decrease of peak (a) during further potential cycling (see Fig. 2a) probably results from Pd dissolution from the alloy. This process causes the depletion of the hydrogen-absorbing component both from the surface and from the bulk of the alloy. Peak (b), which in the case of alloys containing less Pd is the main signal in the hydrogen region at the beginning of the electrochemical treatment, decreases continuously during potential cycling. This effect is accompanied by the splitting into two poorly separated peaks resembling

hydrogen adsorption/desorption peaks on a CV curve for a polycrystalline Pt electrode [18, 24]. Such an evolution of the voltammetric response supports the statement that signal (b) is mainly due to a surface process, namely the oxidation of adsorbed hydrogen, and its decrease reflects the diminution of real surface area of the electrode.

Since the changes in hydrogen peak currents observed during cyclic voltammetry might be affected by the dependence of the rate of hydrogen absorption on alloy composition, in Fig. 5 we present the results of stationary measurements of hydrogen electrosorption carried out for various stages of electrochemical ageing of a Pd–Pt–Rh alloy of composition similar to that presented in Fig. 2a. A comparison of hydrogen oxidation currents in Fig. 5 with CV curves shown in Fig. 2a and alteration of charges presented in Fig. 4a and b confirms the conclusion that the initial increase and subsequent decrease in the height of peak (a) are really caused by the increase/decrease in alloy ability to absorb hydrogen. Under the same conditions a monotonic decline in currents in region (b) is again observed, which is consistent with the mainly surface origin of signal (b), as was stated above.

Conclusions

1. Cyclic voltammograms for Pd–Pt–Rh alloys are generally similar to CV curves characteristic of pure noble metals and their binary alloys, with the easily distinguishable regions of hydrogen sorption/desorption, double layer charging and surface oxidation/oxides reduction. Different alloy compositions lead to CV responses varying with respect to the shape and potential of particular current signals.
2. Both Rh and Pd are dissolved from the alloy during cyclic voltammetry in the oxygen potentials region. The composition changes resulting from selective removal of alloy components are not restricted to the surface but also concern some layers beneath the surface.
3. The procedure of electrochemical ageing influences markedly the shape and height of signals corresponding not only to surface reactions (adsorption/desorption of hydrogen and oxygen), but also to bulk reactions (hydrogen absorption). A positive shift of the oxygen desorption peak mirrors changes in composition of alloy surface becoming more noble. A decrease in currents originating from surface processes reflects lowering of real surface area. Changes in the morphology of alloy surface are confirmed by scanning electron microscope images.
4. Preferential Rh dissolution from the surface as well as from the bulk facilitates hydrogen absorption into the alloy. This may be a result of both removal of the surface layer of Rh (surface changes) and enrichment of the alloy bulk with Pd (bulk changes).
5. Cyclic voltammetry allows for in situ examination of the electrochemical behavior of ternary Pd–Pt–Rh alloys. The complexity of the system makes it difficult to obtain as much quantitative information about the surface state as for binary noble metal systems, although valuable qualitative data are easily available.
6. Selective removal of alloy components during potential cycling experiment allows for in situ preparation of alloy electrodes possessing a variety of adsorption and absorption properties.

Acknowledgements This work was financially supported by Department of Chemistry of Warsaw University and Industrial Chemistry Research Institute.

References

1. Burke LD, Borodzinski JJ, O'Dwyer KJ (1990) Electrochim Acta 35:967
2. Jusys Z, Massong H, Baltruschat H (1999) J Electrochem Soc 146:1093
3. Frelink T, Visscher W, Cox AP, van Veen JAR (1995) Electrochim Acta 40:1537
4. Furuya N, Yamazaki T, Shibata N (1997) J Electroanal Chem 431:39
5. Schmidt TJ, Gasteiger HA, Behm RJ (1999) Electrochem Commun 1:1
6. Podlovchenko BI, Aliua L (1972) Elektrokhimiya 8:460
7. He C, Kunz HR, Fenton JM (1997) J Electrochem Soc 144(3):970
8. Venkataraman R, Kunz HR, Fenton JM (2003) J Electrochem Soc 150(3):A278
9. He C, Kunz HR, Fenton JM (1997) J Electrochem Soc 150(8):A1017
10. Ley KL, Liu R, Pu C, Fan Q, Leyarovska N, Segre C, Smotkin ES (1997) J Electrochem Soc 144(5):1543
11. Liu L, Visvanathan R, Liu R, Smotkin ES (1998) Electrochem Solid-State Lett 1(3):123
12. Urban PM, Funke A, Muller JT, Himmen M, Docter A (2001) Appl Catal A 221:459
13. Napporn WT, Laborde H, Léger JM, Lamy C (1996) J Electroanal Chem 404:153
14. Lima A, Coutanceau C, Léger JM, Lamy C (2001) J Appl Electrochem 31:379
15. Paulus UA, Wokaun A, Scherer GG, Schmidt TJ, Stamenkovic V, Markovic NM, Ross PN (2002) Electrochim Acta 47:3787
16. Shim J, Yoo DY, Lee JS (2000) Electrochim Acta 45:1943
17. Araujo MFA, Rodrigues IA, Tanaka AA (2003) 54th ISE Meeting, Book of Abstracts, p 125, abstract No. 490
18. Woods R (1976) Chemisorption at electrodes. In: Bard AJ (ed) Electroanalytical chemistry, vol 9. Marcel Dekker, New York, pp 2–162
19. Jerkiewicz G (1998) Prog Surf Sci 57:137
20. Lewis FA (1967) The palladium–hydrogen system. Academic Press, New York
21. Sakamoto Y, Ohira K, Kokubu M, Flanagan TB (1997) J Alloys Compd 253:212
22. Thiebaut S, Bigot A, Achard JC, Limacher B, Leroy D, Percheron-Guegan A (1995) J Alloys Compd 231:440
23. Brodowsky H, Husemann H (1966) Ber Bunsenges Phys Chem 70:626
24. Rand DAJ, Woods R (1972) J Electroanal Chem 36:57
25. Capon A, Parsons R (1975) J Electroanal Chem 65:285
26. Kadirgan F, Beden B, Léger JM, Lamy C (1981) J Electroanal Chem 125:89

27. Grdeń M, Paruszewska A, Czerwiński A (2001) J Electroanal Chem 502:91
28. Grdeń M, Piaścik A, Koczorowski Z, Czerwiński A (2002) J Electroanal Chem 532:35
29. Łukaszewski M, Kuśmierczyk K, Kotowski J, Siwek H, Czerwiński A (2003) J Solid State Electrochem 7:69
30. Grdeń M, Czerwiński A, Golimowski J, Bulska E, Krasnodębska-Ostręga B, Marassi R, Zamponi S (1999) J Electroanal Chem 460:30
31. Bolzan A, Martins ME, Arvia AJ (1986) J Electroanal Chem 207:279
32. Perdriel C L, Custidiano E, Arvia A J (1988) J Electroanal Chem 246:165
33. Łukaszewski M, Czerwiński A (2003) Electrochim Acta 48:2435
34. Sakamoto Y, Baba K, Flanagan TB (1988) Z Phys Chem NF 158:223
35. Rand DAJ, Woods R (1972) J Electroanal Chem 35:209
36. Gossner K, Mizera E (1982) J Electroanal Chem 140:47